Cell Reports, Volume *42*

Supplemental information

Selective ablation of primary and paracrine senescent cells by targeting iron dyshomeostasis

Tesfahun Dessale Admasu, Kristie Kim, Michael Rae, Roberto Avelar, Ryan L. Gonciarz, Abdelhadi Rebbaa, João Pedro de Magalhães, Adam R. Renslo, Alexandra Stolzing, and Amit Sharma

Supplemental Figures and Tables

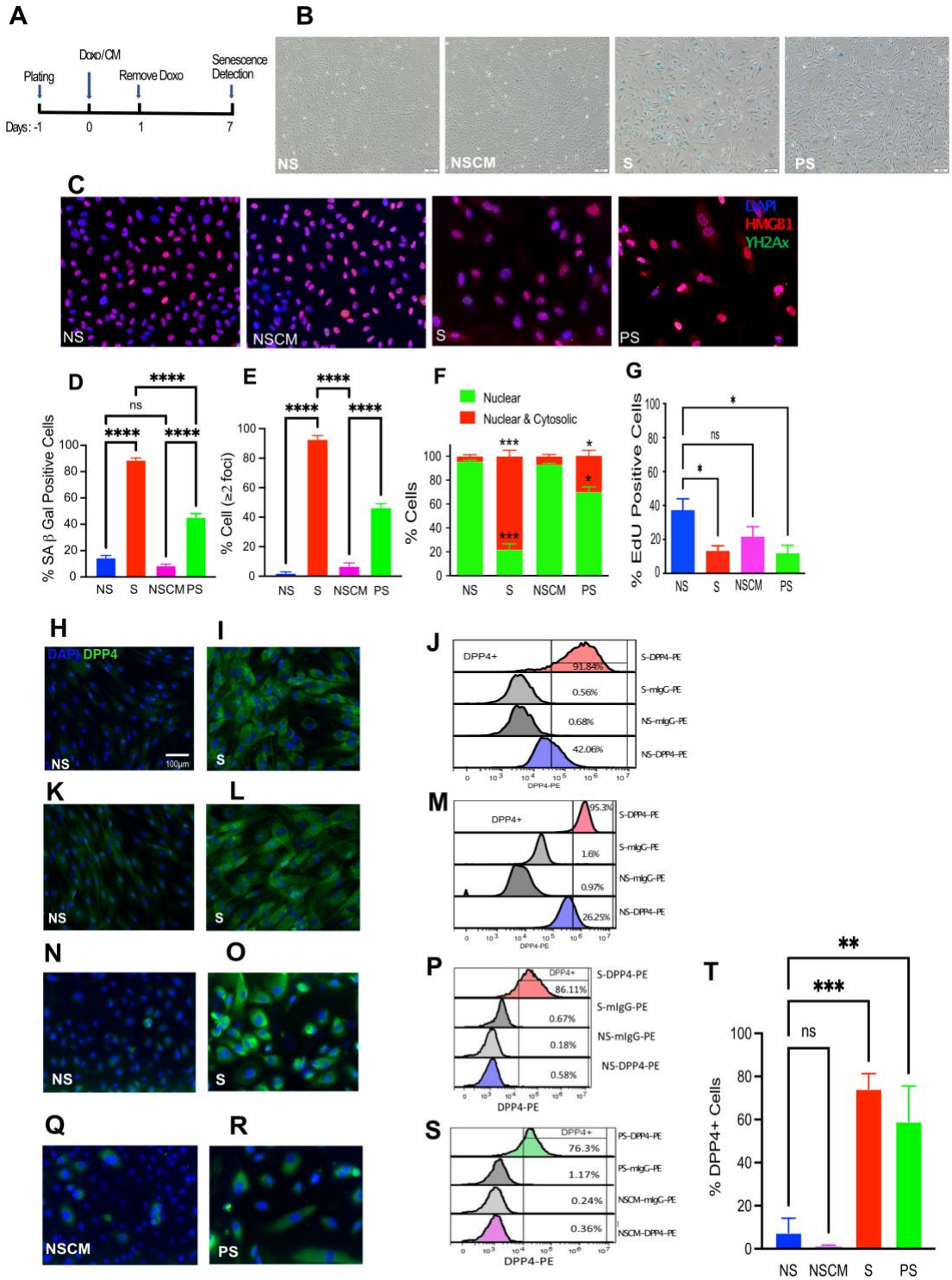

Figure S1. Related to Figure 1. Primary and paracrine senescent cells express DPP4 on their surface.

(A) Flow chart of primary and paracrine senescence induction. (B) Representative images of SA β Gal staining. (C) Representative images of γH2AX and HMGB1 immunofluorescence. (D) Percent of SA β Gal positive cells 7 days after doxorubicin or CM treatment. (E) Quantification of γH2AX foci; cells with two or more foci per nucleus were defined as SCs. (F) HMGB1 relocalizes in SCs. Percentage of cells expressing HMGB1 in the nucleus (green) and nucleus + cytosol (red) was scored. (G) Cell proliferation assay, percentage of Click-it EdU Alexa Fluor 488 positive cells. (H-I) DPP4 immunofluorescence staining in fibroblasts (IMR90). (J) Flow cytometry analysis of DPP4 expression in NS and S IMR90. (K and L) DPP4 immunofluorescence staining in mesenchymal stem cells. (M) Flow cytometry analysis of DPP4 expression in mesenchymal stem cells. (N-O) DPP4 immunofluorescence staining of S and NS ECs. (P) Flow cytometry analysis of DPP4 expression in S and NS ECs. (Q-R) DPP4 immunofluorescence staining of PS and NSCM-treated ECs. (S) Flow cytometry analysis of DPP4 expression in PS and NSCM-treated ECs. (T) Percent of $DPP4^+$ ECs from flow analysis in three donors. Values were presented as mean ± SEM. Comparison was made with one-way ANOVA. Error bars = SEM. *P < 0.05, **P < 0.01, ***P < 0.001, ****P < 0.0001.

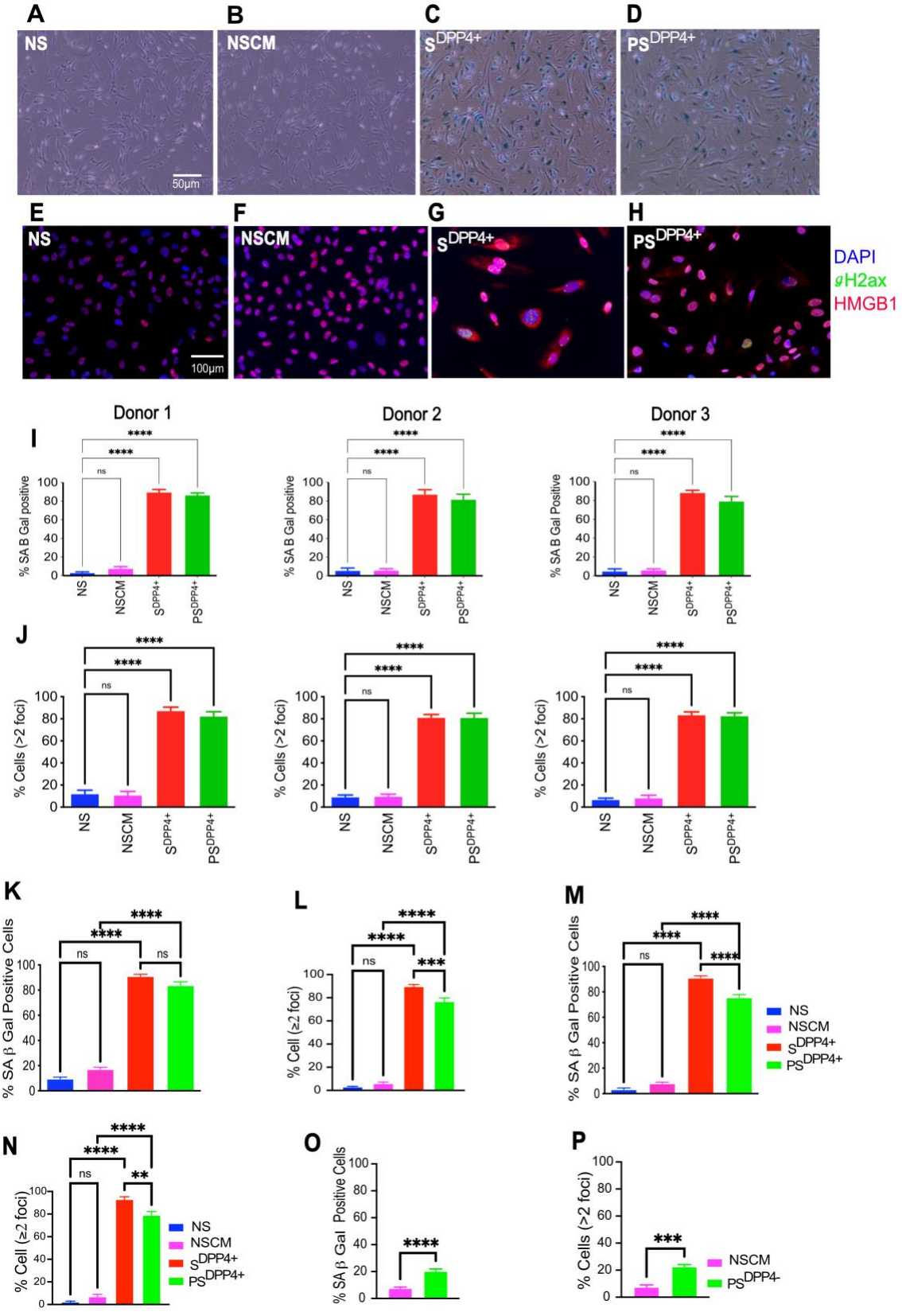
A
B
C
D
NS
NSCM
S DPP4+
PS DPP4+
50µm
E
F
G
H
100µm
DAPI
γH2ax
HMGB1
I
Donor 1
Donor 2
Donor 3
% SA B Gal positive
% SA B Gal Positive
J
% Cells (>2 foci)
K
% SA β Gal Positive Cells
L
% Cell (≥2 foci)
M
N
O
% SA β Gal Positive Cells
P
% Cells (>2 foci)
NS
NSCM
S DPP4+
PS DPP4+
PS DPP4-
ns
**
***
****

Figure S2. Related to Figure 1. Isolation of live SCs using DPP4 as a surface marker. (A-D) Representative images of SA β Gal staining in S^{DPP4+} and PS^{DPP4+} and their respective controls. (E-H) Representative images of γH2AX and HMGB1 staining in S^{DPP4+} and PS^{DPP4+} and their NS controls. Both primary and paracrine SCs were isolated based on DPP4 expression and replated. 24hrs after replating cells were stained for SA β Gal, or γH2AX and HMGB1. (I) Percent of SA β Gal positive cells in S^{DPP4+} and PS^{DPP4+} ECs in three donors. (J) Percent of cells with two or more γH2AX foci in S^{DPP4+} and PS^{DPP4+} ECs in three donors. (K) Percent of SA β Gal positive cells in S^{DPP4+} (irradiated) and PS^{DPP4+} ECs treated with CM from irradiated cells. (L) quantification of γH2AX foci in irradiated S^{DPP4+} and their PS^{DPP4+} ECs. (M) as in (K) for doxorubicin treated IMR90 cells and their paracrine SCs. (N) as in (L) for irradiated IMR90 cells and their paracrine SCs. (O) Percent of SA β Gal positive cells in DPP4- flowthrough paracrine senescent ECs. (P) Percent of cells with two or more γH2AX foci in $DPP4^-$ flowthrough paracrine senescent ECs. Values were presented as mean ± SEM. Comparison was made with one-way ANOVA. Error bars = SEM. **P < 0.01, ***P < 0.001, ****P < 0.0001.

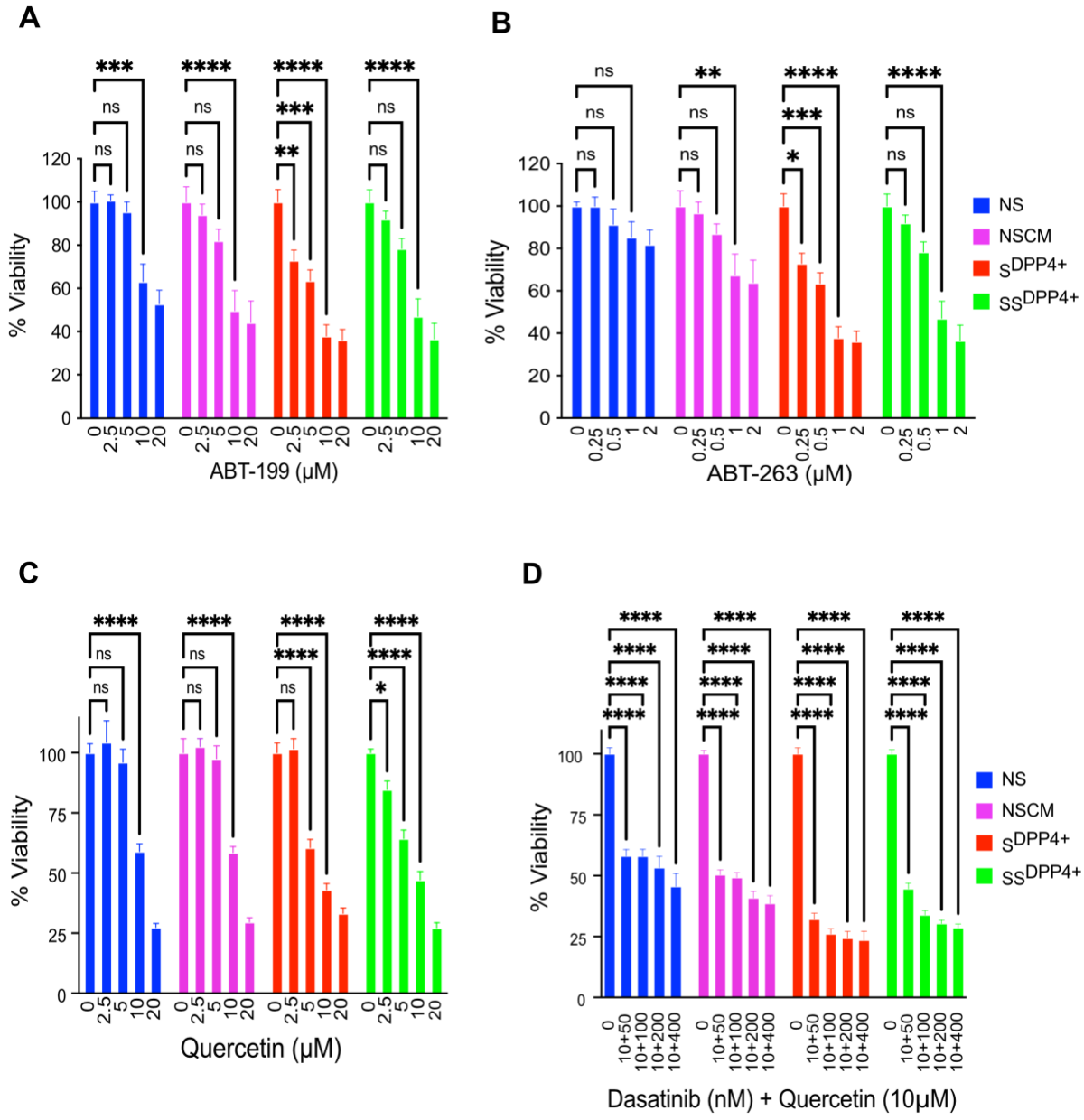
A
B
C
D
% Viability
ABT-199 (μM)
ABT-263 (μM)
Quercetin (μM)
Dasatinib (nM) + Quercetin (10μM)
NS
NSCM
SDPP4+
SSDPP4+
ns
*
**
***
****

Figure S3. Related to Figure 2. PS^{DPP4+} are refractory to senolytic drugs effective against S^{DPP4+}.

(A) Dose optimization of ABT-199. Viability was determined 24hrs after treatment. The same data with Fig. 2B. (B) As in (A) for ABT-263. Viability was determined 48hrs after treatment. The same data with Fig. 2C. (C) As in (A) for Quercetin. Viability was determined 48hrs after treatment. The same data with Fig. 2D. (D) As in (A) for D + Q combination. Viability was determined 48hrs after treatment. The same data with Fig. 2E. (n=3 technical replicates for 3 donors). Comparison was made with two-way ANOVA. Error bars = mean ± SEM. *P < 0.05, **P < 0.01, ***P < 0.001, ****P < 0.0001.

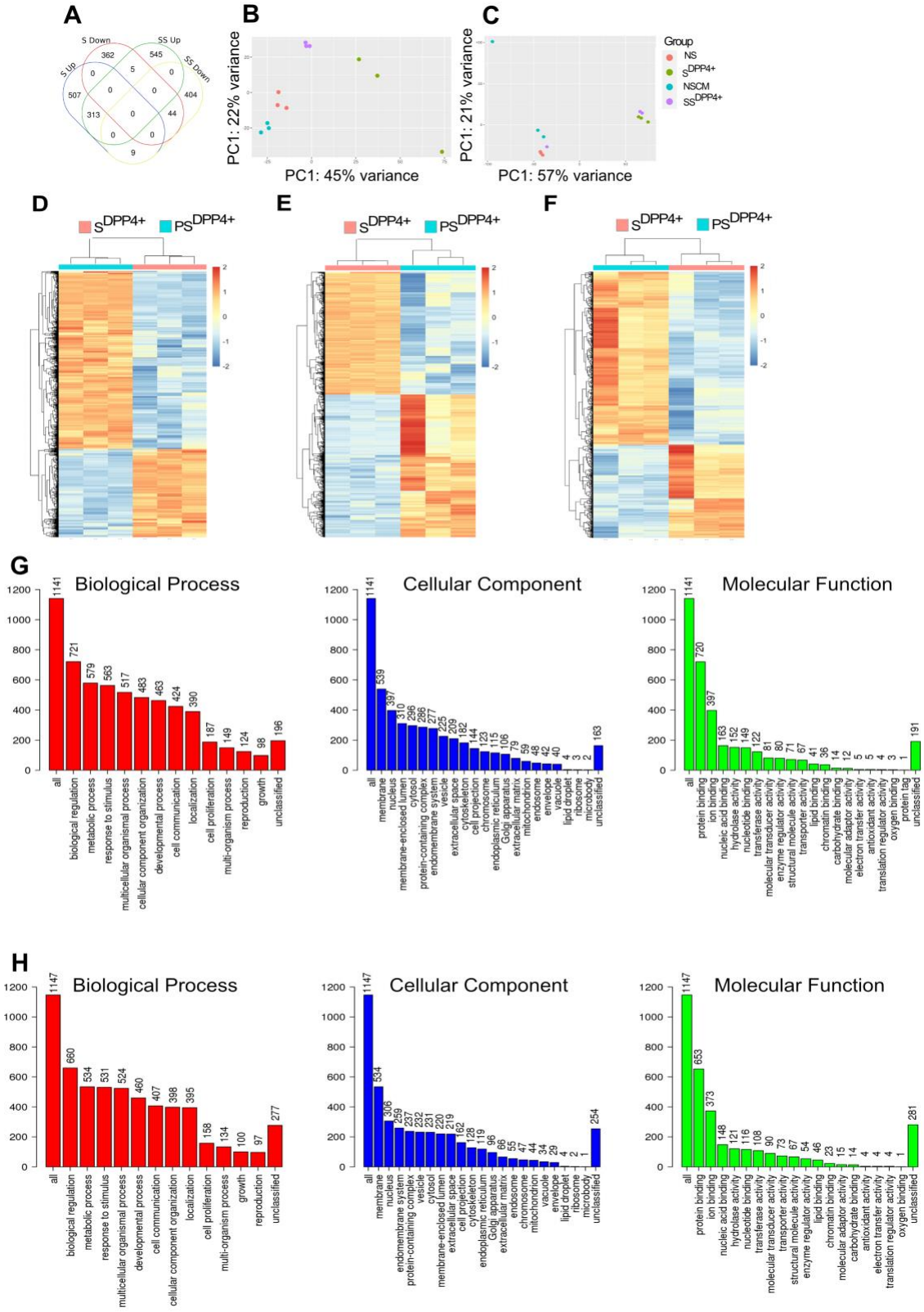
A
S Down
SS Up
S Up
SS Down
362
545
507
404
313
44
9
B
PC1: 22% variance
PC1: 45% variance
C
PC1: 21% variance
PC1: 57% variance
Group
NS
SDPP4+
NSCM
SSDPP4+
D
E
F
SDPP4+
PSDPP4+
G
Biological Process
Cellular Component
Molecular Function
all
biological regulation
metabolic process
response to stimulus
multicellular organismal process
cellular component organization
developmental process
cell communication
localization
cell proliferation
multi-organism process
reproduction
growth
unclassified
membrane
nucleus
membrane-enclosed lumen
cytosol
protein-containing complex
endomembrane system
vesicle
extracellular space
cytoskeleton
cell projection
chromosome
endoplasmic reticulum
Golgi apparatus
extracellular matrix
mitochondrion
endosome
envelope
vacuole
lipid droplet
ribosome
microbody
protein binding
ion binding
nucleic acid binding
hydrolase activity
nucleotide binding
transferase activity
molecular transducer activity
enzyme regulator activity
structural molecule activity
transporter activity
lipid binding
chromatin binding
carbohydrate binding
molecular adaptor activity
electron transfer activity
antioxidant activity
translation regulator activity
oxygen binding
protein tag
H
Biological Process
Cellular Component
Molecular Function

Figure S4. Related to Figure 3. Transcriptome profile of S^{DPP4+} and PS^{DPP4+}.

(A) Venn diagram of DEGs of S^{DPP4+} and PS^{DPP4+}. (B) 2D PCA of S^{DPP4+} and PS^{DPP4+} and NS controls from one donor. PS^{DPP4+} samples were well separated from S^{DPP4+}, NS and NSCM-treated samples. (C) 2D PCA of S^{DPP4+} and PS^{DPP4+} and NS and NSCM-treated controls from one donor. PS^{DPP4+} samples were well separated from S^{DPP4+}, NS and NSCM-treated samples. (D-F) Heat map of the DEGs for S^{DPP4+} and PS^{DPP4+} for three donors. In each donor PS^{DPP4+} were well separated from S^{DPP4+} and clustered together. Heat maps indicate the averages of 3 experiments (n=3 technical replicates for each 3 donors). (G and H) GO term categories using PANTHER classification system for S^{DPP4+} (G) and PS^{DPP4+} (H). GO terms categorized by biological process, cellular component, and molecular function.

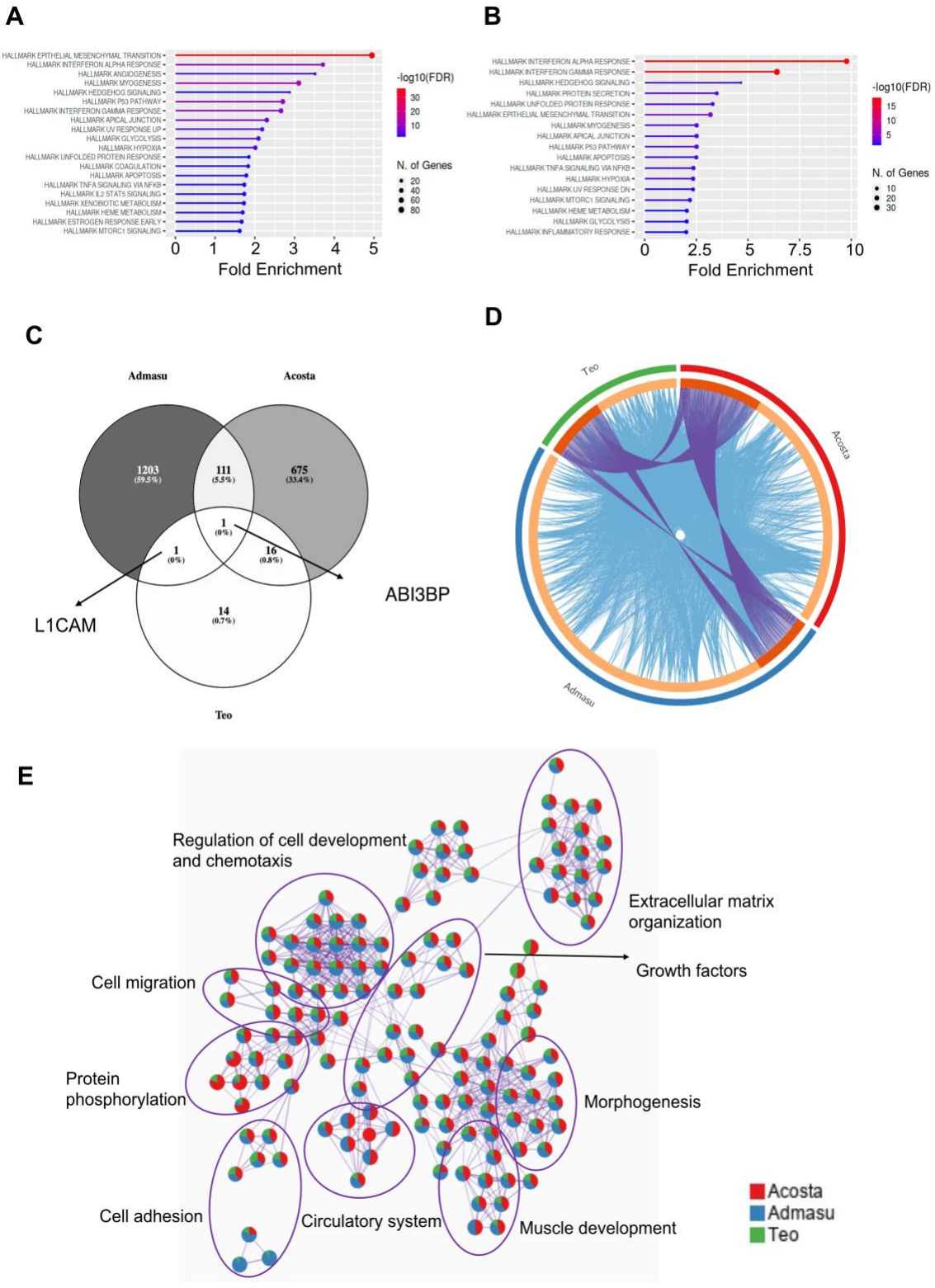
A
HALLMARK EPITHELIAL MESENCHYMAL TRANSITION
HALLMARK INTERFERON ALPHA RESPONSE
HALLMARK ANGIOGENESIS
HALLMARK MYOGENESIS
HALLMARK HEDGEHOG SIGNALING
HALLMARK P53 PATHWAY
HALLMARK INTERFERON GAMMA RESPONSE
HALLMARK APICAL JUNCTION
HALLMARK UV RESPONSE UP
HALLMARK GLYCOLYSIS
HALLMARK HYPOXIA
HALLMARK UNFOLDED PROTEIN RESPONSE
HALLMARK COAGULATION
HALLMARK APOPTOSIS
HALLMARK TNFA SIGNALING VIA NFKB
HALLMARK IL2 STAT5 SIGNALING
HALLMARK XENOBIOTIC METABOLISM
HALLMARK HEME METABOLISM
HALLMARK ESTROGEN RESPONSE EARLY
HALLMARK MTORC1 SIGNALING
0 1 2 3 4 5
Fold Enrichment
-log10(FDR)
30
20
10
N. of Genes
20
40
60
80
B
HALLMARK INTERFERON ALPHA RESPONSE
HALLMARK INTERFERON GAMMA RESPONSE
HALLMARK HEDGEHOG SIGNALING
HALLMARK PROTEIN SECRETION
HALLMARK UNFOLDED PROTEIN RESPONSE
HALLMARK EPITHELIAL MESENCHYMAL TRANSITION
HALLMARK MYOGENESIS
HALLMARK APICAL JUNCTION
HALLMARK P53 PATHWAY
HALLMARK APOPTOSIS
HALLMARK TNFA SIGNALING VIA NFKB
HALLMARK HYPOXIA
HALLMARK UV RESPONSE DN
HALLMARK MTORC1 SIGNALING
HALLMARK HEME METABOLISM
HALLMARK GLYCOLYSIS
HALLMARK INFLAMMATORY RESPONSE
0 2.5 5 7.5 10
Fold Enrichment
-log10(FDR)
15
10
5
N. of Genes
10
20
30
C
Admasu
Acosta
1203
(59.5%)
111
(5.5%)
675
(33.4%)
1
(0%)
1
(0%)
16
(0.8%)
14
(0.7%)
L1CAM
ABI3BP
Teo
D
Teo
Acosta
Admasu
E
Regulation of cell development and chemotaxis
Extracellular matrix organization
Growth factors
Cell migration
Protein phosphorylation
Morphogenesis
Cell adhesion
Circulatory system
Muscle development
Acosta
Admasu
Teo

Figure S5. Related to Figure 3. Transcriptome profile of PS^{DPP4+}.

(A and B) Functional enrichment analysis using WebGestalt for S^{DPP4+} (A) and PS^{DPP4+} (B). DEG's (|LFC| >= 1, P-value < 0.05) was used as an input for GO term analysis. P-value < 0.05, term enrichment > 1.5 were used as a cut of for the GO terms analysis. (C) comparison of the DEGs of PS^{DPP4+} with previously reported DEGs of secondary SCs. (D) Circos plot illustrating overlap of genes differentially expressed in PS^{DPP4+} and previously reported genes by other groups. Purple lines link genes whose transcription is affected by multiple groups. Blue lines link genes affected by one group only, but which fall into the same GO term. A greater number of purple and blue links and longer dark orange perimeter arcs indicate greater overlap between the DEG and GO terms affected. (E) Enrichment network analysis: each term is represented by a circle node, where its size is proportional to the number of input genes fall into that term, and each pie sector is proportional to the number of hits originated from a group. (Parameters: minimum overlap = 3, minimum enrichment = 1.5, p value < 0.01).

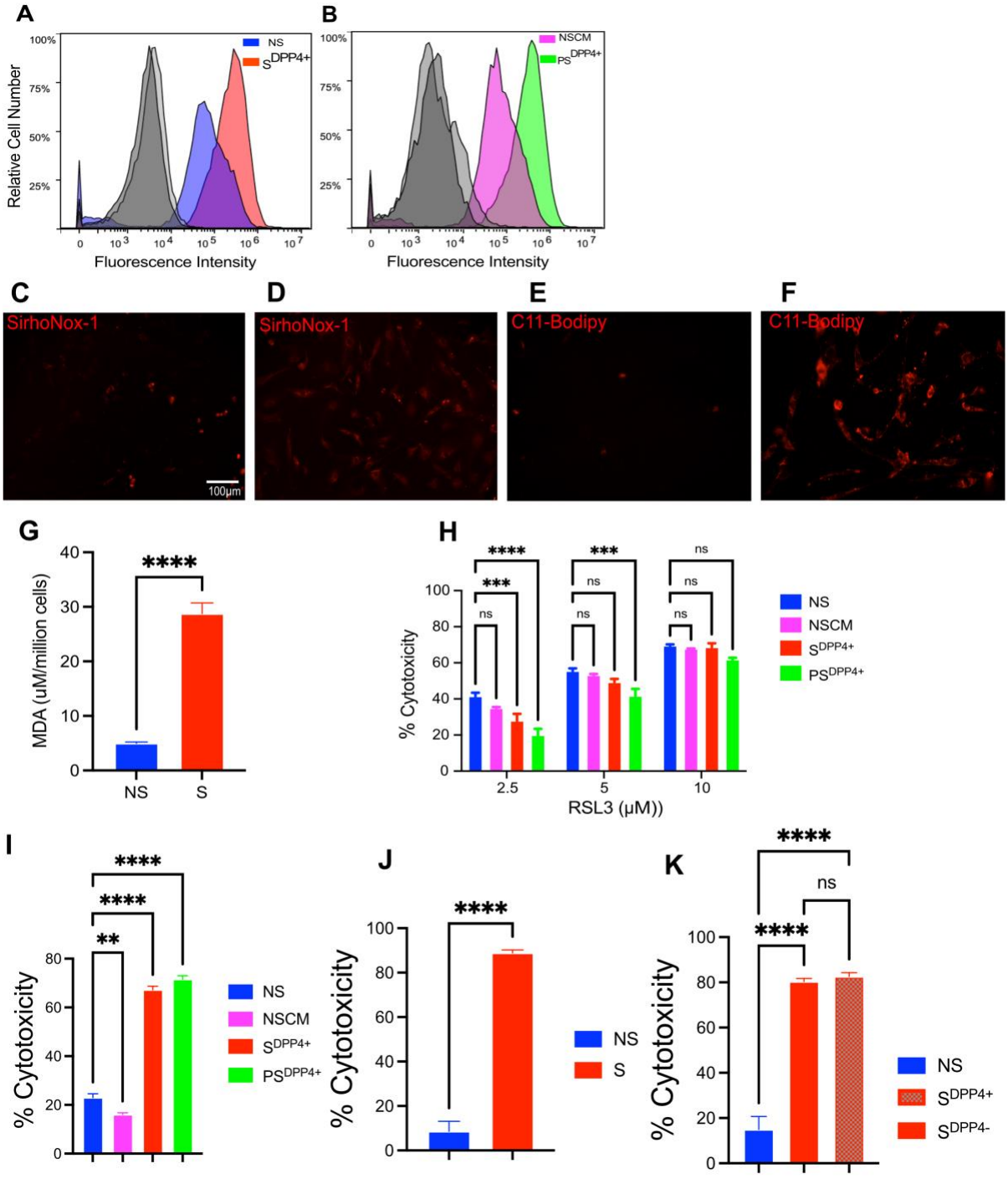
A
B
Relative Cell Number
100%
75%
50%
25%
NS
SDPP4+
NSCM
PSDPP4+
0
10^3
10^4
10^5
10^6
10^7
Fluorescence Intensity
C
D
E
F
SirhoNox-1
C11-Bodipy
100µm
G
MDA (uM/million cells)
****
NS
S
H
% Cytotoxicity
***
ns
2.5
5
10
RSL3 (µM))
NS
NSCM
SDPP4+
PSDPP4+
I
**
J
S
K
SDPP4-

Figure S6. Related to Figure 4-6. Senescent cells have high ferrous iron content and primed to ferroptosis.

(A and B) ferrous iron staining using SiRhoNox-1 in S^{DPP4+} (A) and PS^{DPP4+} ECs (B). (C-D) Representative SiRhoNox-1 based ferrous iron staining in NS (C) and S ECs (D). (E-F) Oxidized lipid staining using C11 Bodipy in NS (E) and S ECs (F). (G) Malondialdehyde (MDA) level in S and NS ECs. (H) Cytotoxicity of RSL3 in in S^{DPP4+} and PS^{DPP4+} ECs. (I) Cytotoxicity of FIN56 in etoposide treated S^{DPP4+} and their PS^{DPP4+} ECs. (J) Cytotoxicity of FIN56 in etoposide treated IMR90 primary SCs. (K) Cytotoxicity of FIN56 in in S^{DPP4+} and S^{DPP4-} IMR90 cells.

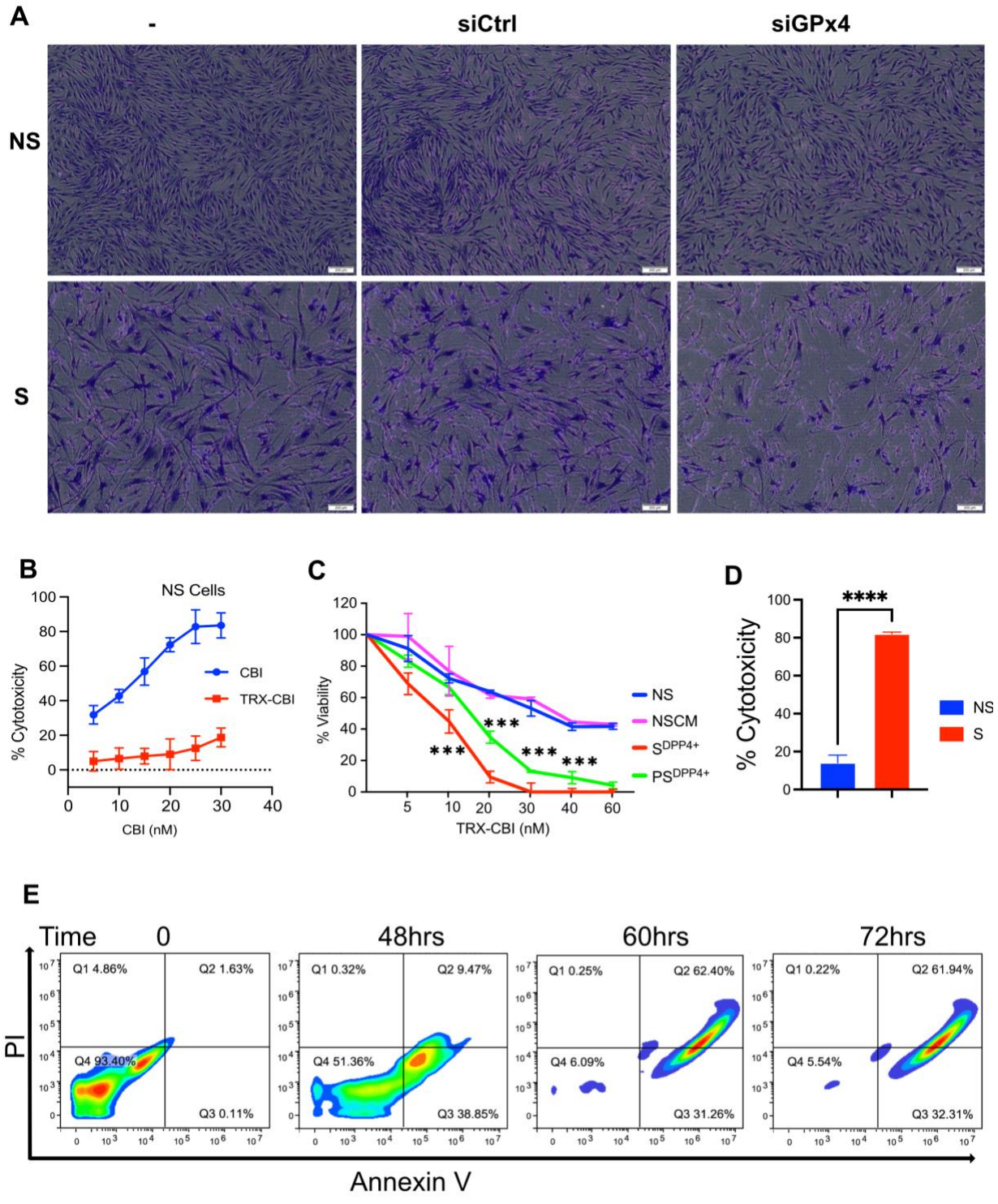
A
-
siCtrl
siGPx4
NS
S
B
NS Cells
% Cytotoxicity
CBI
TRX-CBI
CBI (nM)
C
% Viability
NS
NSCM
S^DPP4+
PS^DPP4+
TRX-CBI (nM)
***
D
% Cytotoxicity
****
NS
S
E
Time
0
48hrs
60hrs
72hrs
PI
Annexin V
Q1 4.86%
Q2 1.63%
Q4 93.40%
Q3 0.11%
Q1 0.32%
Q2 9.47%
Q4 51.36%
Q3 38.85%
Q1 0.25%
Q2 62.40%
Q4 6.09%
Q3 31.26%
Q1 0.22%
Q2 61.94%
Q4 5.54%
Q3 32.31%

Figure S7. Related to Figure 6. Ferrous iron-activatable prodrug as a senolytic approach.
(A) Cytotoxicity of CBI and TRX-CBI in NS ECs. (B) Cytotoxicity of TRX-CBI in S^{DPP4+} and PS^{DPP4+} IMR90 cells. (C) Cytotoxicity of TRX-CBI in etoposide treated senescent IMR90 cells. (D) TRX-CBI induces apoptosis in senescent ECs. SCs were treated with 20nM TRX-CBI and apoptosis were determined by annexin V and PI flow analysis at different time point.